

# **Experimental evaluation of ground motion scaling methods for nonlinear analysis of structural systems**

A.P. O'Donnell,<sup>1</sup> Y.C. Kurama,<sup>2</sup> E. Kalkan,<sup>3</sup> A.A. Taflanidis<sup>4</sup>

<sup>1</sup>Graduate Student, Civil and Environmental Engineering and Earth Sciences, Univ. of Notre Dame, 156 Fitzpatrick Hall, Notre Dame, IN 46556; PH: (617) 797-2311; email: [aodonne1@nd.edu](mailto:aodonne1@nd.edu)

<sup>2</sup>Professor, Civil and Environmental Engineering and Earth Sciences, Univ. of Notre Dame, 156 Fitzpatrick Hall, Notre Dame, IN 46556; PH: (574) 631-8377; email: [ykurama@nd.edu](mailto:ykurama@nd.edu)

<sup>3</sup>Research Structural Engineer, Earthquake Science Center, United States Geological Survey, 345 Middlefield Rd., Menlo Park, CA 94025; PH: (650) 329-5146; email: [ekalkan@usgs.gov](mailto:ekalkan@usgs.gov)

<sup>4</sup>Associate Professor, Civil and Environmental Engineering and Earth Sciences, Univ. of Notre Dame, 156 Fitzpatrick Hall, Notre Dame, IN 46556; PH: (574) 631-5696; email: [a.taflanidis@nd.edu](mailto:a.taflanidis@nd.edu)

## **ABSTRACT**

This paper describes an experimental investigation on the scaling of ground motion records for use in the nonlinear response history analysis of building structures. The study is based on the measured response from small-scale shake-table experiments of nonlinear multi-story building frame structures under ground motion suites that have been scaled using different methods. Four structural configurations with different fundamental periods and lateral strengths are investigated to assess the effectiveness of the scaling methods in reducing the dispersion in the seismic lateral displacement demands of the structures from a total of 720 shake-table tests. Four scaling methods are examined including three methods that depend on a priori knowledge of the properties of the structure being analyzed as well as a method based solely on the properties of the ground motions. The experimental results show that the method based solely on the properties of the ground motions generally produced demand results with less dispersion than the other evaluated scaling methods. However, the methods that rely on prior knowledge of the structure performed better at preserving the benchmark median demands for several of the cases considered.

## **INTRODUCTION**

The task of selecting and scaling an appropriate set of ground motion records is one of the most important challenges for practitioners conducting response history analyses (RHA) for seismic design and risk assessment. Ironically, this is also the single task with the least guidance from current building codes, resulting in the use of mostly subjective choices that can potentially alter the design outcome and increase the amount of uncertainty in the analysis results. For example, according to ASCE 7-10 (2010), the average 5%-damped linear-elastic acceleration response spectrum for a set of design ground motions should not be less than the site-specific design spectrum over the period range from  $0.2T_1$  to  $1.5T_1$ , where  $T_1$  is the fundamental period of the structure being designed. The design value of an engineering demand parameter (EDP)—member deformations, lateral displacements, floor accelerations, etc.—is taken as the average EDP if seven or more records are used in the analysis, or its maximum value over all ground motions if the structure is analyzed for less than seven records (ASCE 7-10 requires a minimum of 3 records). The required number of records prescribed by

ASCE 7 is based on engineering judgment instead of a comprehensive evaluation (Reyes and Kalkan 2011; Haselton 2009).

To demonstrate the challenges for current practice, Figure 1 shows the measured peak roof drift demands,  $\Delta_r$  (i.e., peak lateral displacement,  $D_r$  divided by the height to the roof) for one of the test structures described in this paper (Frame NL2R2) subjected to a suite of 36 ground motion records scaled according to the ASCE 7-10 scaling criteria. The linear-elastic spectral acceleration,  $S_a(T_1)$  of each record at the fundamental period,  $T_1$  of the structure is plotted on the  $x$ -axis. It is clear from the large dispersion in the  $\Delta_r$  demands that if only the peak demand from 3 records are used in design, as allowed by ASCE 7-10, then the design outcome (i.e., over-design, under-design, satisfactory) can be drastically altered depending on the records selected, thus diminishing engineering confidence. Although the use of a large number of records may improve the median EDP estimates, this approach may not be practical. Furthermore, the use of a large number of records does not answer the question of how these records should be scaled for a given design scenario. Thus, there is a need to develop the knowledge to achieve reliable demand estimates from RHA used in seismic design and assessment.

The previous research on ground motion scaling for nonlinear analysis (e.g., Kurama and Farrow 2003; Haselton 2009; Reyes and Chopra 2012; Kalkan and Chopra 2012) has been based solely on numerical simulations with no experimental data available for the validation of the results. The shake-table tests described in this paper form the first experimental investigation to evaluate the accuracy (that is, ability to provide accurate estimates of the median demands as if a much larger set of records were used) and efficiency (that is, ability to minimize the number of records needed to reliably obtain these accurate median demand estimates) of ground motion scaling methods.

## GROUND MOTION RECORDS AND SCALING METHODS

A total of 39 near-fault strong ground motions recorded within 20 km of the causative fault in shallow-crustal tectonic environments were used for scaling and analysis purposes. These records are the same as those listed in O'Donnell et al. (2011). The following five suites of ground motions were developed based on the 39 records:

- GM[Uns] – The unscaled suite of 39 records.
- GM[ASCE7] – The records scaled according to ASCE 7-10 (2010).
- GM[ $S_a(T_1)$ ] – The records scaled to the median  $S_a(T_1)$  of the suite for each structure (Shome et al. 1998).
- GM[MIV] – The records scaled to the median MIV of the suite, where MIV is the maximum area under the acceleration time-history of a record between two consecutive zero acceleration crossings (Kurama and Farrow 2003).
- GM[MPS] – The records scaled based on the Modal Pushover-based Scaling (MPS) procedure (Kalkan and Chopra 2010, 2011).



**Figure 1. Peak  $\Delta_r$  demands for Frame NL2R2.**

Note that three of the scaled records [A-CTR270, PRI000, FOR000; see O'Donnell et al. (2011)] could not be used in the experimental program due to stroke limitations of the shake-table actuator. Thus, the shake-table tests described later were conducted for only 36 records out of the full suite of 39 records. Figure 2 shows the 0.78%-damped linear-elastic acceleration response spectra,  $S_a$  of the 39 ground motion records in each suite, where  $\xi=0.78\%$  corresponds to the measured damping of the test structures in the linear-elastic response range. In addition to the intensity-based scaling of the ground motions, each record was also modified with a length-scale of  $S_L=1/10$  and a time-scale of  $S_T=1/3$  according to the similitude requirements for the small-scale test structures. The GM[MIV] suite was determined by scaling each record to the median [calculated as the geometric mean as described in Cornell et al. (2002)] MIV of the 39 unscaled ground motion records. The GM[ $S_a(T_1)$ ] suite was determined using a similar approach by scaling each record to the median 0.78%-damped  $S_a(T_1)$  of the unscaled suite. However, unlike the GM[MIV] suite, a different GM[ $S_a(T_1)$ ] suite had to be developed for each structure with a different  $T_1$ .

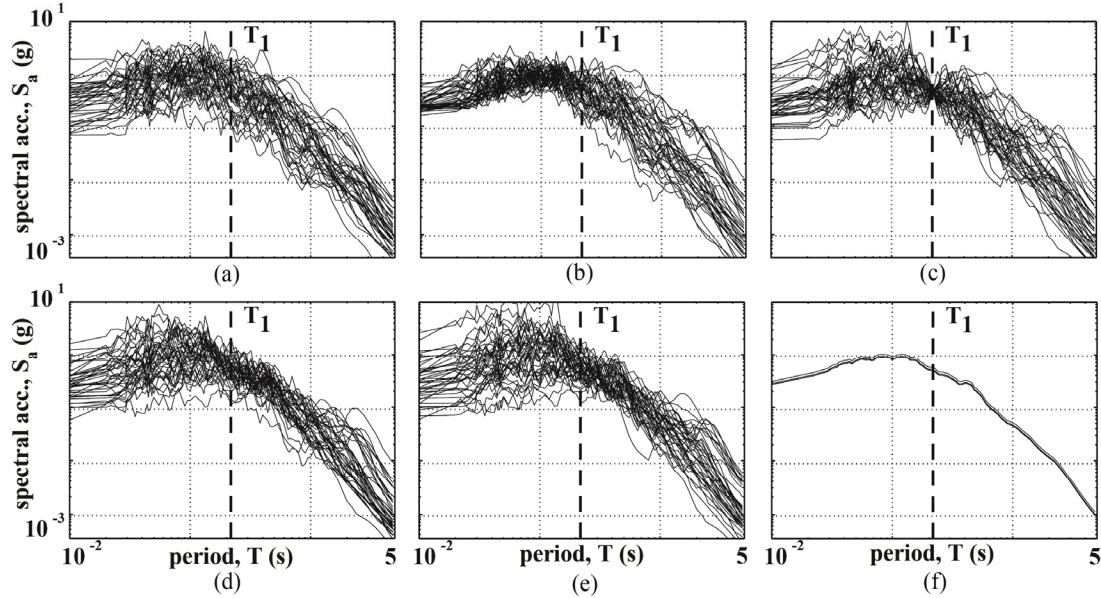


**Figure 2. Linear-elastic acceleration spectra,  $S_a$ :** (a) GM[Uns];(b) GM[ASCE7]; (c) GM[ $S_a(T_1)$ ]; (d) GM[MIV]; (e) GM[MPS]; (f) median spectra of five suites.

In applying the ASCE-7 scaling method, the records were scaled such that the average 5%-damped linear-elastic acceleration response spectrum for the suite was not less than the target median (geometric mean) spectrum of the unscaled records over the period range from  $0.2T_1$  to  $1.5T_1$ . This scaling method utilized 5%-damped spectra (instead of the measured damping) as required by ASCE-7. The median spectrum of the unscaled records (rather than a code-based design spectrum) was used as the target so as not to introduce a bias to the study. A different scaling factor was determined for each record in the GM[ASCE7] suite to minimize the square-root-of-the-sum-of-squares (SRSS) error between the spectrum of the scaled record and the target spectrum within the period range of  $0.2T_1$  to  $1.5T_1$ . Note that the ASCE 7-10 method does not result in a unique scaling factor for each record; various combinations of scaling factors can satisfy the requirement that the mean spectrum of

the scaled records is above the target spectrum over the specified period range (Kalkan and Chopra 2011). An optimization algorithm in Appendix A of Kalkan and Chopra (2010) was used to determine the scaling factors for the GM[ASCE7] suite.

In contrast to the other scaling methods, the *MPS* method (Kalkan and Chopra 2010, 2011) explicitly considers the nonlinear lateral load versus displacement behavior of the structure. The lateral load versus displacement behaviors for the test structures in this research were obtained from monotonic pushover experiments conducted as described later. The scaling factor for each ground motion in the GM[*MPS*] suite was found by matching the peak lateral displacement demand from the nonlinear RHA of an equivalent nonlinear single-degree-of-freedom (SDF) system for the structure (obtained from the pushover load-displacement curve) under the scaled record with the median demand for the equivalent SDF system under the full unscaled ground motion suite. Similar to the  $S_a(T_1)$  and ASCE-7 methods, a different GM[*MPS*] suite was developed for each structure with a different nonlinear lateral load versus displacement behavior. For demonstration purposes, the GM[ $S_a(T_1)$ ], GM[ASCE7], and GM[*MPS*] suites in Figure 2 are shown for scaling based on the measured  $T_1$  and pushover behavior of Frame NL2R2.

The median (geometric mean) value of the scaling factors for the ground motions in each of the five suites from Figure 2 was 1, 0.994, 0.96, 1, and 1.09 for GM[Uns], GM[ASCE7], GM[ $S_a(T_1)$ ], GM[MIV], and GM[*MPS*], respectively. The resulting median response spectrum of the ground motions in each suite is depicted in Figure 2(f), where it can be seen that the median spectra of the different suites are almost identical to one another, only varying in magnitude by at most 9% (in other words, the different scaling methods affect the details of the individual records while the median intensity is mostly preserved).

## TEST STRUCTURES

As shown in Figure 3, the frame structure configuration selected for the experimental investigation was a six-story single-bay system with center-to-center span length of 762 mm and story height of 432 mm. These dimensions correspond to a building length-scale of, approximately,  $S_L=1/10$ . The structure was subjected to the five ground motion suites described previously with a time-scale of  $S_T=1/3$ .

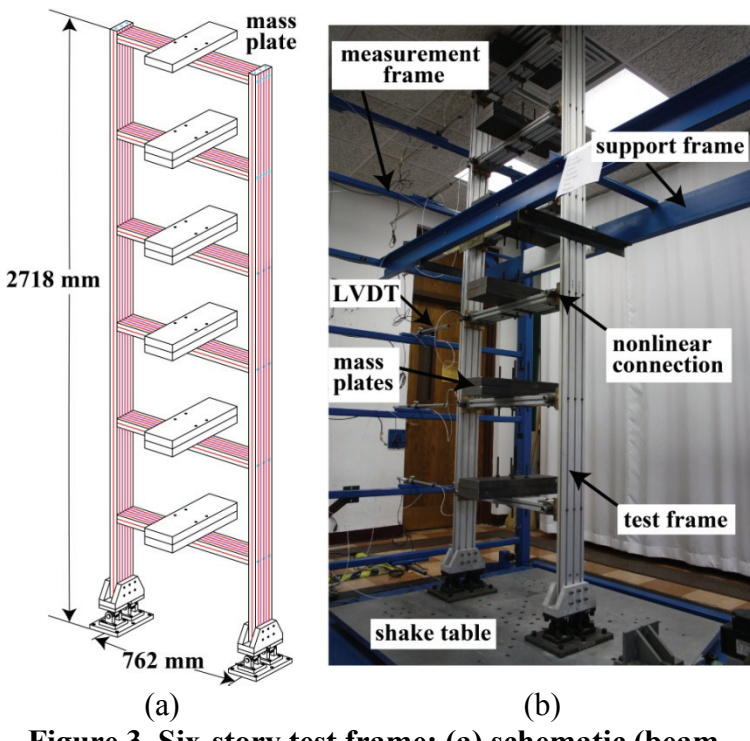


**Figure 3. Six-story test frame: (a) schematic (beam-column connections not shown); (b) test setup.**

The tests were conducted on a medium-size uniaxial shake table that consists of a hydraulic actuator/servo-valve assembly and a hydraulic power supply that drive a 1.2 m by 1.2 m slip table.

To generate structures with different fundamental periods, two different superimposed mass configurations (using 21 kg steel mass plates attached to the midspan of each beam) were investigated. Additionally, the lateral strength of the structure was adjusted, resulting in four frame configurations as follows:

- Frame NL2R2 – two mass plates at each floor level and one plate at the roof, with the structure configured to achieve a lateral strength equal to  $\frac{1}{2}$  of the linear-elastic base shear strength calculated using a design spectral acceleration (corresponding to a response modification factor of  $R=2$ );
- Frame NL2R4 – two mass plates at each floor level and one plate at the roof, with the structure configured to achieve a lateral strength equal to  $\frac{1}{4}$  of the linear-elastic base shear strength from a design spectral acceleration (corresponding to  $R=4$ );
- Frame NL4R2 – four mass plates at each floor level and one plate at the roof, with the structure configured to achieve a lateral strength equal to  $\frac{1}{2}$  of the linear-elastic base shear strength from a design spectral acceleration ( $R=2$ );
- Frame NL4R4 – four mass plates at each floor level and one plate at the roof, with the structure configured to achieve a lateral strength equal to  $\frac{1}{4}$  of the linear-elastic base shear strength from a design spectral acceleration ( $R=4$ ).

To achieve a nonlinear but reusable structure, a connection design utilizing sliding friction interfaces was used at each beam end as shown in Figure 4 and described in O'Donnell et al. (2012). The beam and column members were fabricated from extruded aluminum 6105-T5 alloy (O'Donnell et al. 2011) with a yield strength of 241 MN/m<sup>2</sup> to result in stiffness appropriate with the scale model and adequate strength to prevent yielding of the members. The column bases were constructed with pinned connections.

The linear elastic fundamental period for Frames NL2R2 and NL2R4 was  $T_1=0.22$  s and for Frames NL4R2 and NL4R4 was 0.27 s as computed by the transfer function of the response of the frames to a long duration white noise base excitation. With the selected time-scale of  $S_T=1/3$ , the fundamental periods of the test frames correspond to full-scale periods of  $T_1=0.66$  and 0.82 s, respectively. White noise excitation rather than resonant sine sweep tests were used to determine the structure periods to ensure that the frames remained in the linear-elastic range during these tests (i.e., rotations of the beam-column connections did not occur). The linear-

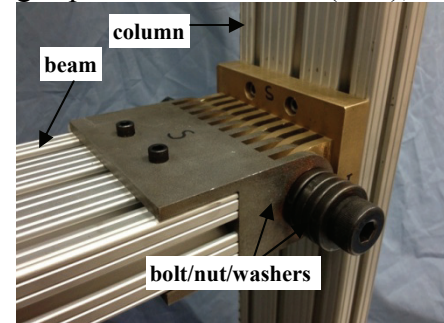


**Figure 4. Nonlinear connection.**

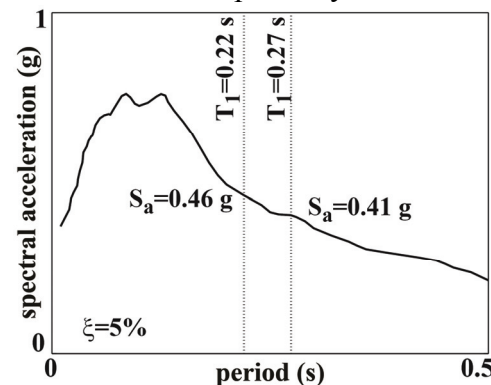


**Figure 5. Design response spectrum.**

elastic base shear demands for the frames were determined by multiplying the total mass of each structure with the design spectral acceleration from the median 5%-damped linear-elastic acceleration response spectrum for the suite of 39 unscaled ground motions, which was used as an unbiased design spectrum. Figure 5 shows this design response spectrum as well as the spectral acceleration values used in the design of each structure. The resulting linear-elastic base shear demands, which correspond to  $R=1$  as presented in Table 1, were then divided by the response modification factors of  $R=2$  and  $R=4$  to determine two design base shear strengths,  $V_{bd}$  representing varying degrees of nonlinearity (with  $R=4$  corresponding to a weaker structure and therefore greater nonlinearity). Note that the use of 5%-damping in design as compared to the measured 0.78%-damping for the structures resulted in lower strengths (using a 0.78%-damped design spectrum, the  $V_{bd}$  values in Table 1 would correspond to  $R=2.93$  and  $5.85$  for Frames NL2R2 and NL2R4, respectively, and  $R=2.85$  and  $5.69$  for Frames NL4R2 and NL4R4, respectively).

The beam-column connection moment strengths,  $M_{cm}$  to result in the design base shear strengths,  $V_{bd}$  for the structures were determined by conducting monotonic pushover tests on frame configurations with varying connection strengths. As described in O'Donnell et al.

(2011), these pushover tests were conducted by holding the 4<sup>th</sup> floor of the frame stationary while slowly displacing the base laterally using the shake table. The connection moment strengths for all 12 connections were kept constant. Between each test, the shoulder bolt in each connection was loosened, the structure brought back to plumb, and the connection bolts re-tightened to the desired torque. As shown in Figure 6(a), a linear trend was observed between the connection moment strength,  $M_{cm}$  and the base shear strength,  $V_{bd}$  of the frame.

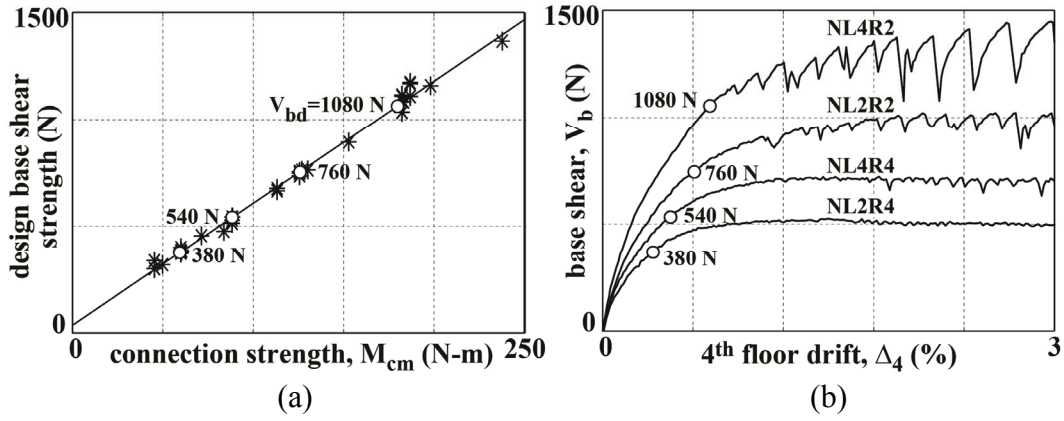


**Figure 6. Connection and frame strengths:** (a)  $M_{cm}$ - $V_{bd}$ ; (b)  $V_b$ - $\Delta_4$ .

The required connection moment strength,  $M_{cm}$  to achieve the design base shear strength,  $V_{bd}$  for each of the four frame configurations is shown by the  $\circ$  markers in Figure 6(a) and listed in Table 1. As can be seen from the base shear,  $V_b$  versus 4<sup>th</sup> floor drift,  $\Delta_4$  results in Figure 6(b), the transition from the linear-elastic to post-yield behavior of the structures did not occur at a distinct yield point. Thus, the

design base shear strength for each structure was determined at a characteristic yield point (○ markers) by dividing the maximum base shear with an assumed overstrength factor of 1.4.

Since each frame configuration was designed for use under a large number of shake table tests, it was imperative that the structure be reusable and repeatable such that each test started from the same initial conditions with the structure possessing the same properties from test to test. In other words, while the behavior of the structure was allowed to go into the nonlinear range during testing under each ground

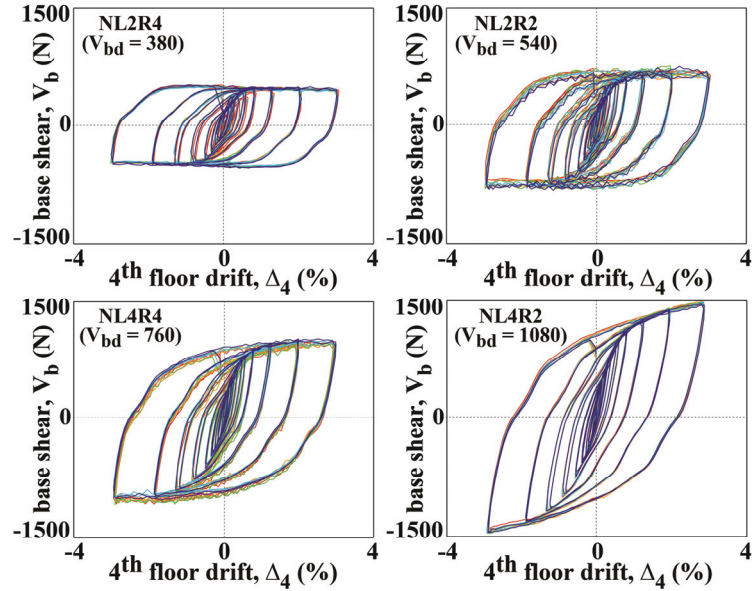


**Figure 7. Repeated reversed-cyclic  $V_b$ - $\Delta_4$  behaviors (five tests for each frame).**

motion, the initial properties (i.e., lateral stiffness, period, damping) were required to remain invariant between the tests. Before the structures were excited dynamically, a series of static reversed-cyclic tests were conducted to observe whether the behavior remained repeatable and symmetrical when the frame was pushed in both directions. Figure 7 shows the hysteretic base shear,  $V_b$  versus 4<sup>th</sup> floor drift,  $\Delta_4$  behavior of each frame under five repeated reversed-cyclic tests. Similar to the monotonic pushover tests, the shoulder bolt in each beam-column connection was loosened after each reversed-cyclic test, the structure was brought back to plumb, and the connection bolts were re-tightened to the desired torque. The hysteresis plots show that the structures exhibited excellent repeatability. It can also be seen that the stick-slip behavior of the nonlinear connections during the monotonic testing of Frame NL4R2 [as indicated by the jagged  $V_b$ - $\Delta_4$  curve beyond the attainment of the design strength in Figure 6(b)] did not occur during reverse-cyclic testing, possibly due to the alternating directions of the connection rotations.

## SHAKE TABLE TEST RESULTS

The four different frame configurations were subjected to a total of 720 shake-table tests. The displacements of the table and each floor of the structure were measured using seven, free, unguided LVDTs anchored between the structure and a fixed measurement frame (Figure 3). The data was collected at a rate of 200 samples per second, resulting in close-to-simultaneous excitation and response measurements.

The peak roof drift,  $\Delta_r$  demands from the five suites of 36 ground motions for each structure are plotted in Figure 8 against  $S_a(T_1)$  and  $MIV$ . A good correlation can be seen between  $\Delta_r$  and  $MIV$ , indicating that the  $MIV$  scaling method may be effective in reducing the dispersion in the  $\Delta_r$  demands as investigated further below.

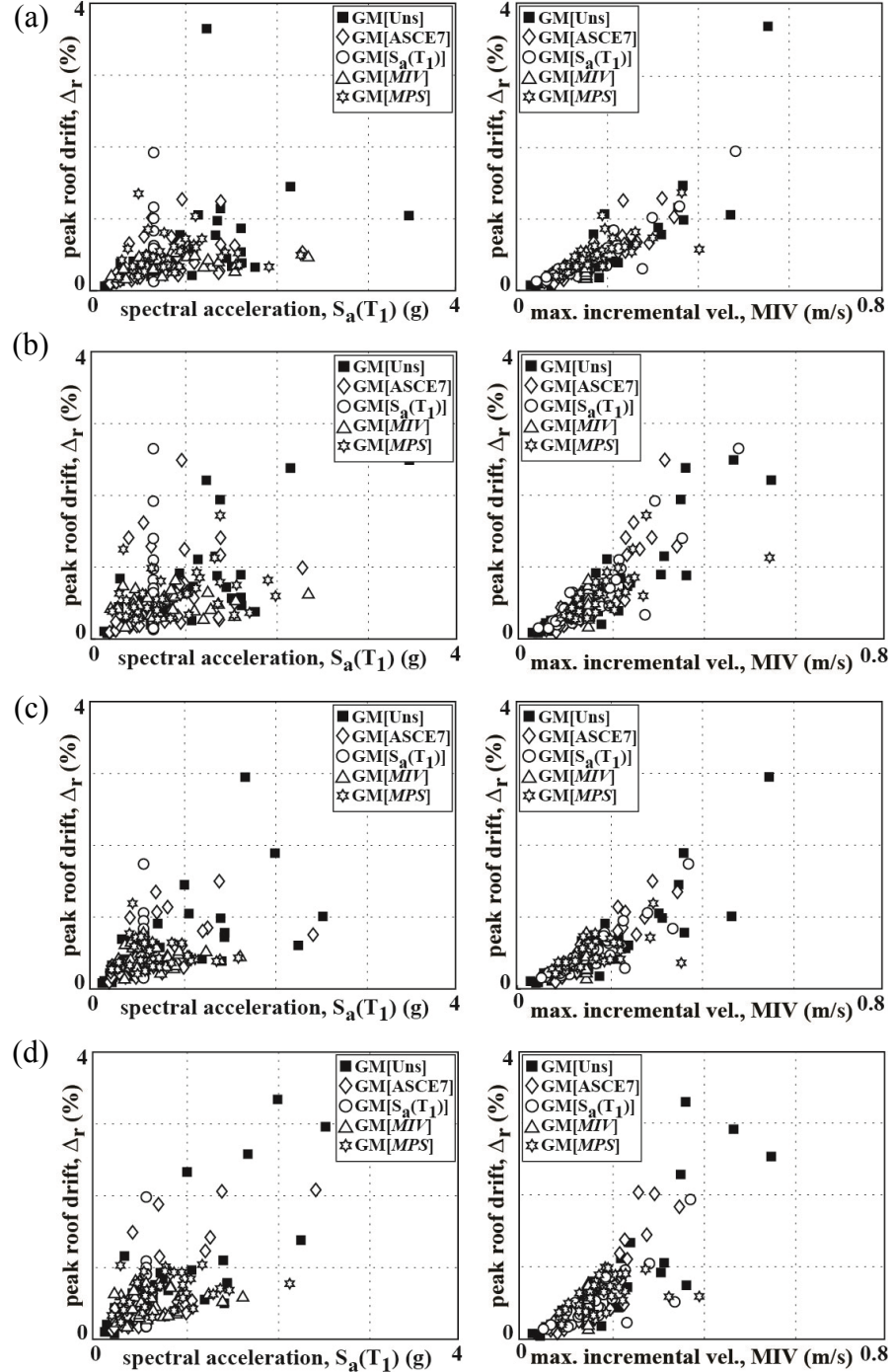


**Figure 8.** Peak roof drift,  $\Delta_r$  demands plotted against  $S_a(T_1)$  and  $MIV$ : (a) Frame NL2R2; (b) Frame NL2R4; (c) Frame NL4R2; (d) Frame NL4R4.

The median [calculated as geometric mean; see Cornell et al. (2002)] peak roof drift,  $\hat{\Delta}_r$  of the unscaled suite of 36 ground motions was assumed to be the benchmark median roof drift demand,  $\hat{\Delta}_{r,BK}$  for each structure. The error in preserving this benchmark demand was calculated for each of the four scaling

methods by dividing the median for each scaled suite,  $\hat{\Delta}_{r,SM}$  by the benchmark median and subtracting 1 from this ratio as,  $E(\hat{\Delta}_r) = (\hat{\Delta}_{r,SM}/\hat{\Delta}_{r,BK}) - 1$ . As shown in Figure 9(a), the error  $E(\hat{\Delta}_r)$  illustrates whether a given scaling method is more likely to under estimate (negative value) or over estimate (positive value) the benchmark median roof drift demand. Additionally, the coefficient of variation (COV) of the peak roof drift demands for each structure under each ground motion suite are shown in Figure 9(b) and listed in Table 2. The COV measure, defined as the ratio between the sample standard deviation and the sample mean, is used to assess the effectiveness of the scaling methods in reducing the dispersion in  $\Delta_r$ .

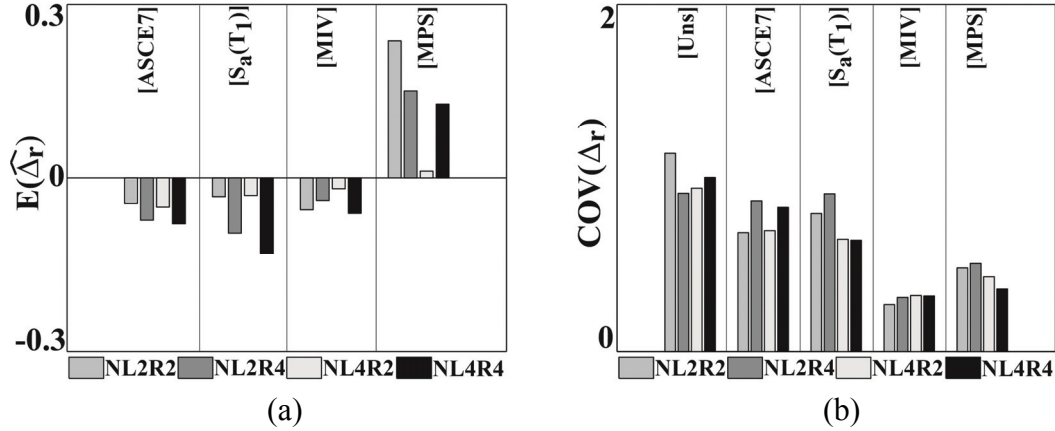


**Figure 9. Peak roof drift demand,  $\Delta_r$  for Frames NL2R2, NL2R4, NL4R2, and NL4R4; (a) error,  $E(\hat{\Delta}_r)$ ; (b) dispersion,  $COV(\hat{\Delta}_r)$ .**

**Table 2. Summary results for peak roof drift demand,  $\Delta_r$**

Frame	GM[Uns]		GM[ASCE7]		GM[S <sub>a</sub> (T <sub>1</sub> )]		GM[MIV]		GM[MPS]	
	$\hat{\Delta}_r$ (%)	COV( $\hat{\Delta}_r$ )	$E(\hat{\Delta}_r)$	COV( $\hat{\Delta}_r$ )	$E(\hat{\Delta}_r)$	COV( $\hat{\Delta}_r$ )	$E(\hat{\Delta}_r)$	COV( $\hat{\Delta}_r$ )	$E(\hat{\Delta}_r)$	COV( $\hat{\Delta}_r$ )
NL2R2	0.373	1.142	-0.044	0.686	-0.032	0.796	-0.055	0.269	0.237	0.479
NL2R4	0.480	0.911	-0.073	0.868	-0.095	0.908	-0.039	0.309	0.151	0.505
NL4R2	0.427	0.941	-0.050	0.698	-0.030	0.648	-0.019	0.321	0.012	0.428
NL4R4	0.531	1.002	-0.079	0.832	-0.130	0.642	-0.061	0.318	0.128	0.358

Note: MIV method performed better than the results in shaded cells.

It can be seen that for all of the cases studied, the *MIV* scaling method consistently performed better than the other methods with regard to minimizing the dispersion in the peak roof drift demand,  $\Delta_r$ . Furthermore, the dispersion in  $\Delta_r$  remained relatively constant between the four structures when using the *MIV* method, but showed greater differences between the structures when using the other scaling methods. With respect to accuracy as measured using  $E(\hat{\Delta}_r)$ , the *MIV* scaling method performed better than the other evaluated methods for most of the cases investigated (gray shaded cells in Table 2), only performing second best in accuracy for Frames NL2R2 and NL4R2. This suggests that for the structures tested, the relative performance of the *MIV* scaling method improved with respect to the accuracy of the evaluated methods as the nonlinearity of the structure was increased.

Additionally, the peak inter-story drift demand,  $\delta_m$  was calculated as the maximum magnitude inter-story drift over the height of each structure under each

ground motion (Figure 10 and Table 3). Again, the *MIV* scaling method was the best method with regard to minimizing the dispersion in  $\delta_m$ . However, with regard to the error,  $E(\hat{\delta}_m)$  in preserving the benchmark median inter-story drift demand, the *MIV* method was outperformed by the *MPS* method for Frames NL2R2 and NL2R4, and by the  $S_a(T_1)$  method for Frames NL2R2, NL4R2, and NL4R4. These results also demonstrate the merits of the *MPS* method, since this method was not only the second best at minimizing dispersion in the peak roof and inter-story drift demands, but it was also comparatively good at preserving the median peak drift demands in a conservative manner (i.e., safer but potentially not as economical).

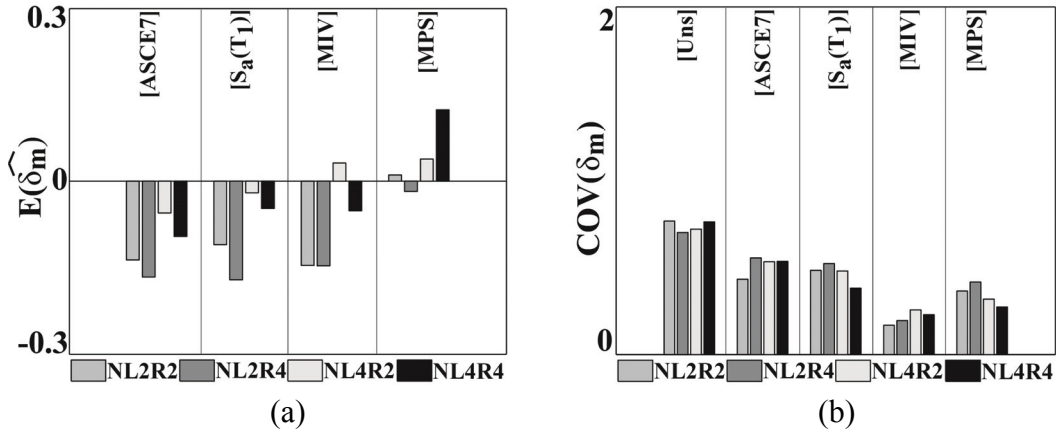


**Figure 10.** Peak inter-story drift demand,  $\delta_m$  for Frames NL2R2, NL2R4, NL4R2, and NL4R4; (a) error,  $E(\hat{\delta}_m)$ ; (b) dispersion,  $COV(\delta_m)$ .

**Table 3. Summary results for peak inter-story drift demand,  $\delta_m$**

Frame	GM[Uns]		GM[ASCE7]		GM[ $S_a(T_1)$ ]		GM[MIV]		GM[MPS]	
	$\hat{\delta}_m$ (%)	COV( $\delta_m$ )	$E(\hat{\delta}_m)$	COV( $\delta_m$ )						
NL2R2	0.846	0.769	-0.138	0.431	-0.110	0.482	-0.147	0.167	0.011	0.364
NL2R4	0.847	0.703	-0.167	0.553	-0.172	0.520	-0.148	0.194	0.018	0.414
NL4R2	0.901	0.723	-0.055	0.531	-0.020	0.478	0.031	0.255	0.038	0.317
NL4R4	0.875	0.764	-0.096	0.533	-0.047	0.379	-0.051	0.227	0.125	0.272

Note: *MIV* method performed better than the results in shaded cells.

## SUMMARY AND CONCLUSIONS

This paper describes an experimental evaluation of four selected ground motion scaling methods [ASCE-7,  $S_a(T_1)$ , *MIV*, and *MPS*] for use in nonlinear response history analysis of building frame structures. The general experimental setup and features of four 1/10-scale six-story nonlinear test frame configurations are presented, along with the identification of the static and dynamic properties of the structures. The scaling methods are evaluated by determining the dispersion in the peak lateral roof and inter-story drift demands of the test frames, as well as the accuracy in the median peak drift demands as compared with the benchmark median peak drift demands from the unscaled suite of records. The results show that the *MIV* scaling method generally performed better than the other three scaling methods in minimizing the dispersion in the peak drift demands. However, with regard to the error in preserving the benchmark median drift demands, the *MIV* method was

outperformed by the *MPS* method and the  $S_a(T_1)$  method for several of the cases considered. The results also demonstrated the merits of the *MPS* method, since this method was not only the second best at minimizing dispersion in the peak drift demands, but it was also comparatively good at preserving the median peak demands in a conservative manner.

It should be noted that among the scaling methods considered, the *MIV* method is the only method that can be applied independent of the properties of the structure being analyzed (e.g., period, damping, lateral strength). Potential errors resulting from inaccuracies in the modeling and analysis of the structure make the design application of the ASCE-7,  $S_a(T_1)$ , and *MPS* methods more uncertain than the *MIV* method. Furthermore, using the *MIV* method, any changes in the structure properties throughout the design process would not require the scaling of the ground motions to be iterated. The biggest disadvantage for the implementation of the *MIV* method in current seismic design procedures is the lack of tools to estimate the mean annual frequency of exceedence of *MIV* and tools to estimate the attenuation of *MIV*. Thus, there is currently no accepted method to determine the probability of exceedence of a certain *MIV* level at a given site. Future research is needed in these areas before the *MIV* scaling method can be used in practice.

## ACKNOWLEDGEMENTS

This research is funded by the National Science Foundation (NSF) under Grant No. CMMI 0928662. The support of Dr. K.I. Mehta, NSF Program Director, and Dr. M.P. Singh, former NSF Program Director, is gratefully acknowledged. The authors would also like to acknowledge the following individuals: Paulo Bazzurro, University Institute for Superior Studies (IUSS); Sigmund Freeman, Wiss, Janney, Elstner Associates, Inc.; Bob St. Henry, NEFF Engineering; Vladimir Graizer, U.S. Nuclear Regulatory Commission; Farzad Naeim, John A. Martin and Associates, Inc.; and Thomas Sabol, Englekirk & Sabol Consulting Structural Engineers, Inc. The opinions, findings, and conclusions in the paper are those of the authors and do not necessarily reflect the views of the organizations or individuals acknowledged.

## REFERENCES

- ASCE (2010). "Minimum design loads for buildings and other structures." American Society of Civil Engineers, ASCE Standard No. ASCE/SEI 7-10, Reston, VA.
- Cornell, C.A., Jalayer, F., Hamburger, R.O. and Foutch, D.A. (2002). "Probabilistic basis for 2000 SAC federal emergency management agency steel moment frame guidelines." *J. of Structural Engineering*, 128(4), 526-533.
- Haselton, C. (2009). "Evaluation of ground motion selection and modification methods: Predicting median interstory drift response of buildings." Pacific Earthquake Engineering Research (PEER) Center, California State University: Chico, CA.
- Kalkan, E. and Chopra, A.K. (2012). "Evaluation of modal pushover-based scaling of one component of ground motion: Tall buildings." *Earthquake Spectra*, 28(4), 1469-1493.
- Kalkan, E. and Chopra, A.K. (2011). "Modal-pushover-based ground motion scaling procedure." *J. of Structural Engineering*, 137(3), 289-310.

- Kalkan, E. and Chopra A.K. (2010). "Practical guidelines to select and scale earthquake records for nonlinear response history analysis of structures." U.S. Geological Survey Open-File Report, 1068, 126.
- Kurama, Y. and Farrow, K. (2003). "Ground motion scaling methods for different site conditions and structure characteristics." *Earthquake Engineering & Structural Dynamics*, 32(15), 2425-2450.
- O'Donnell, A., Beltsar, O., Kurama, Y., Kalkan, E., and Taflanidis, A. (2011). "Evaluation of ground motion scaling methods for analysis of structural systems." *ASCE Structures Congress*, Las Vegas, NV.
- Reyes J. and Chopra A.K. (2012). "Modal pushover-based scaling of two components of ground motion records for nonlinear RHA of structures." *Earthquake Spectra*, 28(3), 1243-1267.
- Reyes, J. and Kalkan, E. (2011). "Required number of records for ASCE/SEI 7 ground motion scaling procedure." U.S. Geological Survey Open-File Report, 1083, 34.
- Shome, N., Cornell, C., Bazzurro, P., and Carballo, J. (1998). "Earthquakes, records, and nonlinear responses." *Earthquake Spectra*, 14(3), 469-500.